Order−Disorder Transition in the Electroactive Polymer Poly(3-dodecylthiophene)

Kang C. Park and Kalle Levon*

Department of Chemical Engineering, Chemistry, and Materials Science, Polytechnic University, Six Metrotech Center, Brooklyn, New York 11201

Received September 6, 1996; Revised Manuscript Received March 7, 1997[⊗]

ABSTRACT: Electrical conductivity is greatly dependent on the quality and degree of crystallinity in semiconjugated polymers. We have investigated the order formation in electrically conducting poly(3-alkylthiophenes) by combining the uses of thermal analysis and optical microscopy. Initially, we were able to observe a bimodal endothermic melting point using differential scanning calorimetry (DSC). Then, using a slow cooling cycle from the melt state with immediate reheating, it was shown that the two melting points are separate phenomena and depend on the thermal history. A single melting point was observed when the sample was cooled to 120 °C and annealed for 1 h. Optical microscopy was then applied for the same conditions. A thermochromic change was observed immediately. This change has been related to changes in chain conformation as the chain planarity increases with the decrease of thermal energy. With the annealing at 120 °C a formation of red dot-like domains could be seen. The formation of these domains was related to the above mentioned single high-temperature melting point. This observation is the first visual observation of the order formation in poly(alkylthiophenes) and also the first evidence of thermochromism taking place by an interchain mechanism such as crystallization. The reason for our observation is the very narrow thermal condition used in the experiments. In further experiments we notice further thermochromic change in the background, indicating a further ordering process that is related to the second endothermic melting point observed in the thermal analysis experiments. Our experiments support the earlier findings of two different ordered phases in poly(alkylthiophenes).

I. Introduction

Electroactive polymers have a wide range of potential applications in electrochromic devices,[1] light-emitting diodes,[2] nonlinear optical materials,[3] *etc.*, of which properties are greatly dependent on the structural features at the molecular level. It has become essential to understand the relationship between molecular structure and electronic properties and the relationship between morphological behaviors and electrical properties of these materials. The structure[4,5] and thermo- and solvatochromism[6,7] of the electroactive polymer poly(3-alkylthiophene) have been extensively studied because the alkylation[8,9] of these electroactive polymers has provided the desired solubility and processibility due to the reduction of strong interactions between main chains and due to the increase in flexibility.

Many studies have accounted for thermo- and solvatochromism on the molecular level. The origin of the thermochromism and solvatochromism has been considered as a result of the interruption of conjugation caused by a generation of twists (disruption of planarity). These twists, which were called "conformons", effectively divide the polymer into subpolymers having a distribution of smaller conjugation lengths. The conformons, which are affected by temperature and solvent power, are taken as the cause of the continuous shift of the main absorption peak. A poly(3-hexylthiophene) solution in chloroform displays a color change from yellow to magenta with the addition of a poor solvent or after cooling to a low temperature.[6] It has also been found that the aggregation (microcrystallization) of P3ATs can occur only after the single chain conformational change has occurred. It was concluded that the two coexisting phases are polymer in solution and polymer in microcrystallized aggregates and that the transition is fundamentally a single chain phenomenon. Inganäs *et al.* also reported thermochromic and solvatochromic effects in the soluble conductive polymer poly(3-hexylthiophene): thin solid films of the polymer change color with a change in temperature, and the color of solutions of the polymer can be changed by varying the composition of the solvent.[7] They observed that optical absorption of good solvents is similar to that of thin solid films at higher temperatures, while in poor solvents, absorption features are similar to those found in solid films at lower temperatures. The presence of a multiphase was also suggested on the basis of the disappearance of the second shoulders at 2.21 eV before the disappearance of the first shoulders at 2.04 eV in the optical spectrum when the film was heated and on the basis of the absence of a true isosbestic point in the temperature dependent spectra.

Qian related the behavior of poly(alkylthiophenes) to block copolymers.[5b] The random distribution of oriented conjugated segments (blocks) was used as the explanation for the lack of birefringence. Thus a block copolymer behavior can be used as a general and informative model for the poly(alkylthiophenes). The order−disorder transition of flexible polymers has been well established both experimentally and theoretically.[10,11] The ensemble of molecular configurations that produces the minimum overall free energy, G, represents the equilibrium state in a block copolymer melt.[12] In general, this criterion differs from the condition for equilibrium in homopolymer mixtures because block copolymers are single-component systems that cannot phase separate. When $\chi > 0$, a decrease in A−B segment−segment contacts in an A−B diblock copolymer reduces the system enthalpy H. This process can occur locally, segregating A and B blocks. The segregation is opposed by the associated loss in system entropy that derives from (1) localizing block−block joints at interfaces and

[⊗] Abstract published in *Advance ACS Abstracts,* May 1, 1997.

S0024-9297(96)01322-8 CCC: $14.00

(2) stretching the chains in order to maintain a uniform density (stretching a polymer chain reduces its conformational entropy). Diblock copolymer entropy is inversely proportional to N, or $S \sim N^{-1}$, and it is the product χN that controls the state of segregation. For $\chi N \ll 10$, entropic factors dominate and diblock copolymers exist in a spatially homogeneous state. Increasing N or χ shifts the free energy balance and leads to the development of local composition fluctuations on a scale proportional to the polymer radius-of-gyration. When $\chi N \approx 10$, a delicate balance exists between entropic and energy effects. Increasing this parameter further induces a first-order transition to an ordered state. In this case entropically favored but energetically costly curved and disordered microstructures are exchanged for a periodic mesophase. Increasing χN further leads to sharper microdomain boundaries as the number of A−B segment−segment contacts decreases at the expense of additional chain stretching. In the limit $\chi N \gg 10$, energy factors dominate, and the ordered microstructures are characterized by narrow interfaces and nearly flat composition profiles. This phase transition has been known as the order−disorder transition (ODT).

Various soluble π-conjugated polymers, which include the polydiacetylenes,[13,14] and polysilanes[15−17] have been reported to exhibit a rod-to-coil transition behavior in the dilute solutions. These systems appear to exhibit single macromolecule transitions which are independent of polymer concentration over many orders of magnitude in the dilute region. In addition to the dilute solution case, true order−disorder transitions have been observed in neat solid films of both the polydiacetylenes[18] and the polysilanes.[19] At high temperatures the films are amorphous, and the polymer molecules are in a disordered state. Cooling leads to rod-like polymers arranged in a semicrystalline fashion. The conformational changes in both films and solutions are accompanied by large spectroscopic changes indicative of a major modification of the polymer's electronic structure at the transition. Several researchers[13,20,21] have suggested that, similar to biopolymers, the transition is driven by intramolecular hydrogen bonding which stabilizes the factor for the polydiacetylenes but not the polysilanes and poly(3-alkylthiophenes). A statistical mechanical theory for the order−disorder transition of conjugated polymers in dilute solutions and neat amorphous films was proposed by Schweizer.[22,23] The theory was developed in detail for π-conjugated polymers (polyenes and polydiacetylenes) in dilute solutions, and it made a significant number of qualitative and quantitative predictions. However, theoretical understanding of the conjugated polymer phenomena is minimal, and the molecular origin of the observed phenomena is still not completely understood.

In our previous research we have investigated the side-chain crystallization, layer formation, and crystallization kinetics of poly(3-dodecylthiophene) from the melt state.[24] Interestingly, a double transition before the isotropization temperature was observed. This additional transition could be related to the formation of a nematic-like phase in which the side chains are highly disordered but the main chains maintain their arrangement. This has motivated us to continue the study on the thermal behavior of P3DDT. In this paper, the thermal behavior of P3DDT was systematically studied using a differential scanning calorimeter and optical microscope to gain more information on the additional endothermic peak and to investigate which factor is most critical for the thermochromism of P3DDT in the solid state.

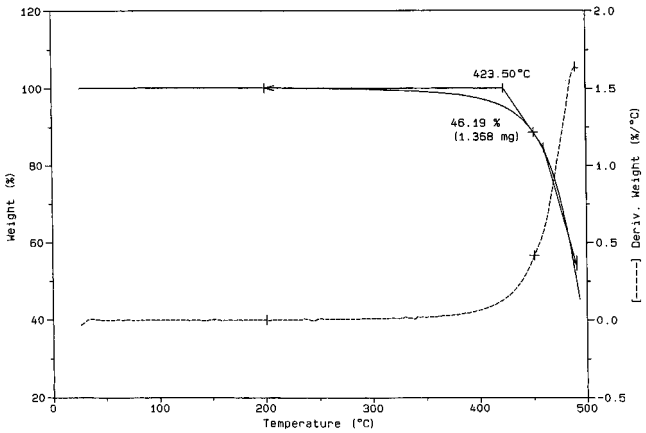

Figure 1. TGA thermogram of poly(3-dodecylthiophene).

II. Experimental Section

The poly(3-dodecylthiophene) substituted in the 3-position by *n*-dodecyl was prepared by oxidative polymerization using $FeCl_3$ as an oxidant. The detailed procedure and the molecular weights and molecular weight distribution of the P3DDT sample were reported in our previous paper.[25] The film of P3DDT was cast on a glass slide from chloroform solution and dried at ambient conditions. The as-cast films were a deep red-brown color and homogeneous when observed through the optical microscope. A Nikon F2 optical microscope was used to study the morphological change of P3DDT with respect to annealing time and temperature. The maximum heating temperature was chosen as 175 °C for the P3DDT samples on the basis of the thermal stability defined from thermogravimetric analysis (Figure 1). At this temperature, it is possible to achieve a homogeneous melt state and to remove any previous thermal history without thermal degradation. A cover glass was placed on the film to prohibit direct contact with air. The samples were heated to 175 °C and held at 175 °C for 5 min to achieve the homogeneous melt and then quenched to a predetermined temperature. The formation of structures was followed by a controlled annealing time as the samples were held at these predetermined temperatures in a Mettler hot stage (FP82) with a central processor (FP80). The thermal transition of P3DDT was also studied by using a Perkin-Elmer TAS7 differential scanning calorimeter with a cooling unit. Each sample, usually 10 mg in weight, was placed in a sealed aluminum pan, and the measurements were carried out in a nitrogen atmosphere. For the isothermal experiments, a new sample was utilized for each crystallization temperature. All the samples were first heated to 175 °C for 5 min and then cooled rapidly (cooling rate, 300 °C/min) to the required crystallization temperature, T_c. After being held at T_c for a predetermined crystallization time, t_c, the samples were reheated from T_c to 175 °C at a rate of 10 °C/min. A Phillips ADP 3720 X-ray generator was used for the WAXD experiments. The point focus beam was monochromatized to Cu Kα with a graphite crystal. The X-ray source, an XRG 3100 generator, utilized a Cu Kα target with generator settings of 40 kV and 20 mA.

III. Results

The thermal behavior of P3DDT was first analyzed by differential scanning calorimetry (DSC). DSC thermograms of P3DDT samples which were heated and cooled cyclically between −40 and +175 °C at a rate of 10 °C/min are shown in Figure 2. The difference between the first and the second heating curves shows a large effect of previous history. The second heating curve shows a single glass transition temperature at about −16 °C, a bimodal lower transition region cover-

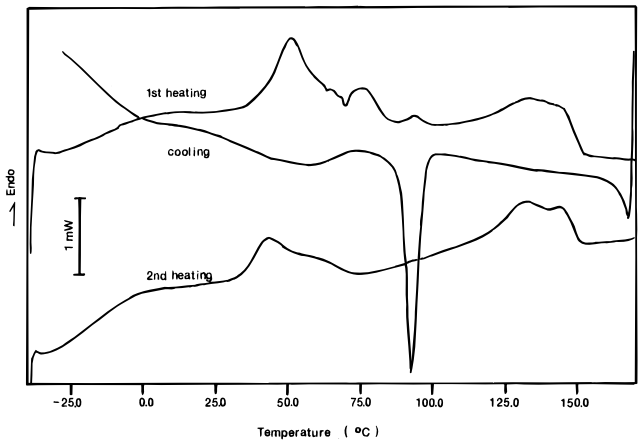

Figure 2. DSC thermograms of poly(3-dodecylthiophene) with a heating and cooling rate of 10 °C/min.

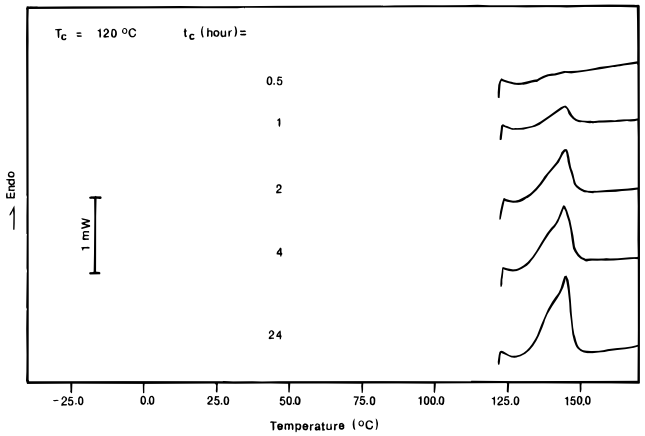

Figure 3. DSC heating curves for samples crystallized at 120 °C for different times.

ing the temperature range of about 30−75 °C, and double endothermic processes having peak temperatures of 133 and 140 °C. The lower transition range indicates the melting of the side-chain crystals, and its broad shape represents a large distribution of the degree of packing in the crystals. The bimodal shape may imply that two packing features, which are determined by the main-chain arrangement, exist. The structural features of the ordered phase could be described with a smectic-like layered arrangement of the chains in which the distance between the main chains is determined by the side-chain length and the degree of interdigitation. The layers are organized in three-dimensional packing, and the side chains may form hexagonal paraffin-like crystals within the layers. Side-chain crystallization has also been shown to occur between side chains in amorphous systems without the layer formation. The relative intensities of these two ordered parts are dependent on the thermal history of the samples.

The thermal behavior of P3DDT was investigated in detail in the temperature region between 75 and 150 °C in order to obtain understanding of the double endothermic processes in the high-temperature region. Figure 3 shows how the melting peak changed with respect to the annealing times. The sample was heated to 175 °C for 5 min, quenched to 120 °C with a cooling rate of 300 °C/min, and then held at this temperature for the different controlled periods of time. Endotherms could not be observed when the annealing time was shorter than 30 min. After 60 min, a single endothermic peak corresponding to the melting temperature of the P3DDT appeared, and this endotherm became larger as annealing times were increased.

To visualize this process, the same thermal procedure was followed under the optical microscope and the optical micrographs are shown in Figure 4. Figure 4a shows that the color of the sample film was yellow at 175 °C. Figure 4b shows that the color of the sample changed from yellow to reddish brown as it was cooled from 175 to 120 °C and then kept at 120 °C for 1 h. This color change will be called the "A" process hereafter. It implies that the electronic structure of the P3DDT chains has been altered from a high band gap to a lower band gap, which can be directly related to changes in chain conformation. The sample with a yellow color at 175 °C has short segments of a π-conjugated conformation. As the temperature decreased from 175 to 120 °C, the chain planarity increased due to a decrease of the thermal energy. The fundamental mechanism of the "A" process is intrachain.

Simultaneously, red dot-like structures began to appear. After an annealing time of 2 h, the red dot-like structures were clearly evident, with a further increase of the annealing times, the growth of the domains continued (Figure 4d), and eventually the domains overlapped (Figure 4e). Figure 4f shows that the morphology of the sample annealed at 120 °C for 24 h is homogeneous and the grain boundaries cannot be detected in the overlapped samples. The series of micrographs shows clearly that the morphology is dependent on annealing times. The process of developing the red dot-like structures will be called the "B" process hereafter. The development of the red dot structures during the "B" process occurs in the same time range as the development of the endothermic processes observed in the DSC experiments. The melting peaks become larger as the red dot structures grow. This indicates that the red dot structures developed during the "B" process, as shown in Figure 4, form a crystalline phase. This was also confirmed by X-ray experiments.

At this point, it is worth noting that the conformational changes are accompanied by large spectroscopic changes, which are indicative of a major modification of the polymer's electronic structure at the transition. As the polymers become ordered, the degree of electron delocalization increases, and hence the polarizability associated with the delocalized electrons of the P3DDT also increases. The arrangement due to interchain interactions can increase the planarity of the main chains and promote the $\pi-\pi$ interchain conjugation so that the conjugation length increases two-dimensionally, in the main-chain direction and in the interchain direction, which is perpendicular to the main-chain axis.

Until now, thermochromism and solvatochromism have been explained by the intrachain mechanism, which deals primarily with backbone conformational changes: the polymer backbone is divided into subpolymers having a distribution of smaller conjugation lengths as the temperature or solvating power of the solvent increases. However, our experimental data now show that thermochromism may also take place by an interchain mechanism such as the crystallization or arrangement of the main chains. For example, at 120 °C, the P3DDT chains began to crystallize slowly by a nucleation growth mechanism. The crystallization increased the chain planarity by an interchain mode so that the color of the P3DDT in the dot structure shifted toward a deeper red color. The sample which was

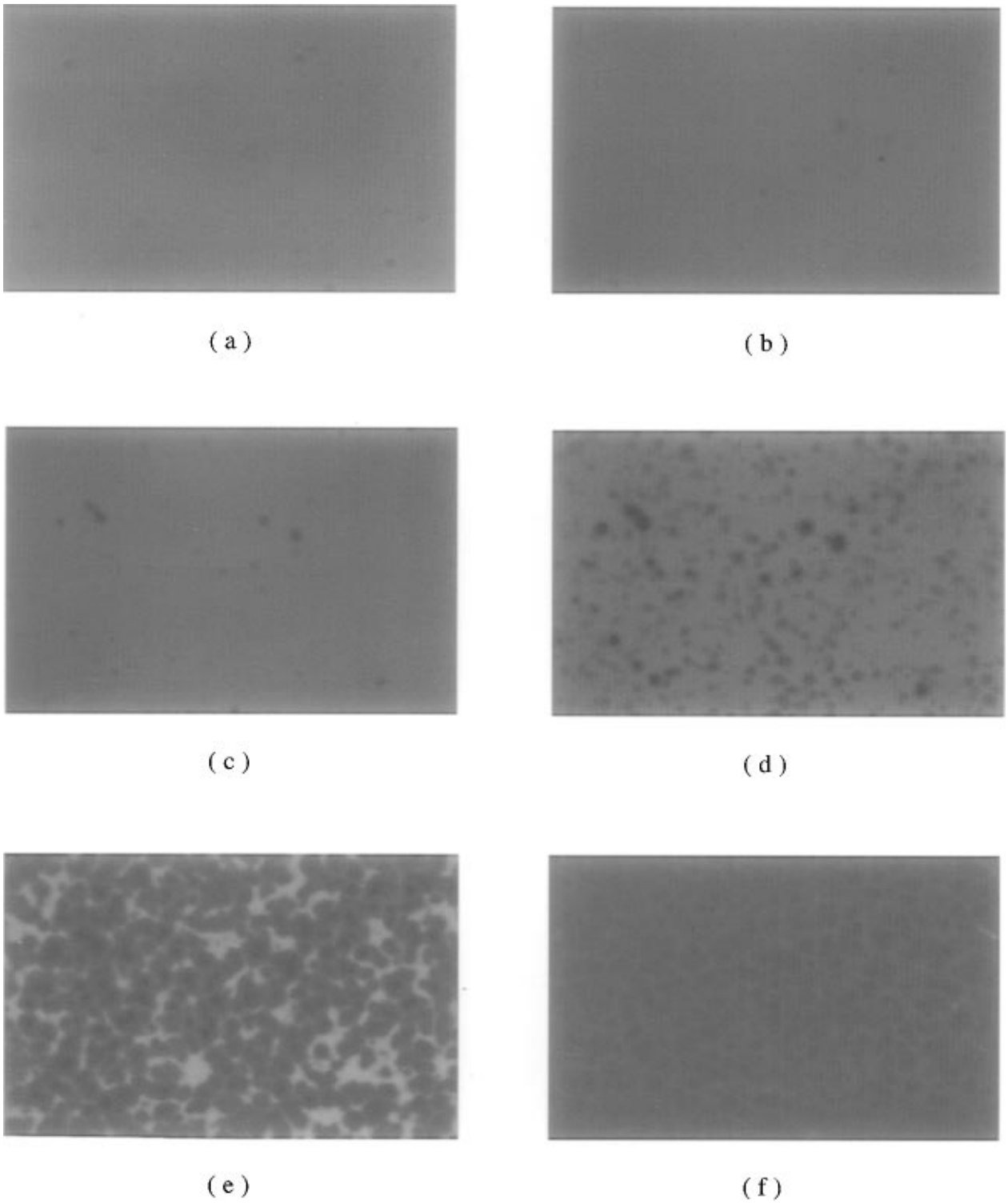

Figure 4. Optical micrographs of poly(3-dodecylthiophene) film crystallized at 120 °C for different times (magnification, ×300): (a) at 175 °C; (b) 1 h; (c) 2 h; (d) 4 h; (e) 8 h; (f) 24 h.

annealed at 120 °C actually has two phases, the crystalline phase with the red dot-like structures and the amorphous background, and the ratio between these phases is dependent on the annealing times.

Our data prove that the thermochromism at 120 °C is induced by two mechanisms. First, the chain planarity increases due to conformational changes by the decrease of thermal energy in the "A" process. Then the crystallization of the main chains in the "B" process further increases the chain planarity. As discussed in the Introduction, Rughooputh *et al.* proposed, on the basis of their spectroscopic data, that aggregation and/or microcrystallization is certainly involved in the thermochromism of the P3ATs.[6] Specific support and confirmation of this interpretation of thermochromism comes from the observation of similar spectral changes on removal of the solvent by evaporation, and from the observation of precipitation of partially crystalline material. They concluded that the two coexisting phases are polymer in solution and polymer in microcrystallized aggregates. In the case of dilute solution, there have been reports about the independence of concentration on thermochromism.[13] Far below the critical concentration, only one phase of the polymer

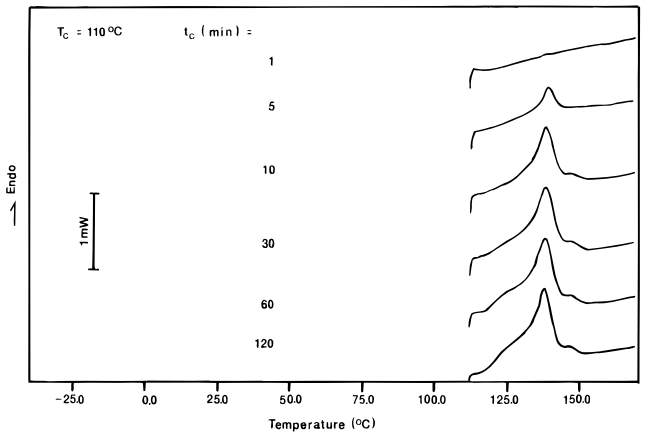

Figure 5. DSC heating curves for samples crystallized at 110 °C for different times.

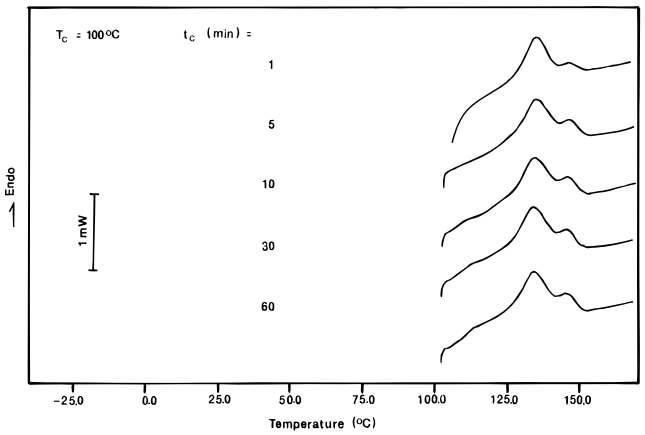

Figure 6. DSC heating curves for samples crystallized at 100 °C for different times.

solution exists in spite of temperature variation because the solution is so dilute that the aggregation boundary cannot be controlled by thermal energy. However, a dependence of concentration on thermochromism near the critical concentration exists because it is possible for the polymer chains to aggregate above the critical concentration when the thermal energy is controlled. The concentration range is critical when thermochromism is discussed in solution, and it is strongly dependent on the solvating power of solvents.

Systematic studies were extended to temperatures of 110, 100, and 90 °C, to investigate the double peaks at 133 and 140 °C and determine their relationship with the morphological changes. Figure 5 shows how the melting peak varies with respect to annealing times of the sample at 110 °C for different periods of time. The sample which was annealed at 110 °C for 1 min did not show any melting peak, while the sample which was annealed for 5 min began to show a melting peak. The longer the annealing time, the larger the melting peak. The samples annealed at 110 °C for 5 min began to develop the red dot structures. As the annealing time was increased, more red dot structures developed, as shown in Figures 8a. However, the sample annealed for 30 min, presented in Figure 8b, shows a color change of the whole phase. This background color change will be called the "C" process. There was no further change in the morphology for the longer annealing time. At this temperature the "C" process, which was not observed at 120 °C due to the fast growth of the "B" process, began to be competitive with the "B" process. As the annealing temperature decreased from 120 to

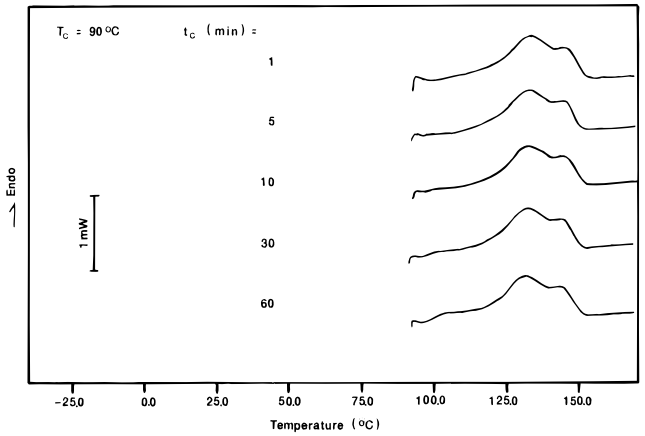

Figure 7. DSC heating curves for samples crystallized at 90 °C for different times.

110 °C, the sample had a broader range in the degree of crystallinity than that at 120 °C, the rate of color changes became faster, and the red dot structures were smaller and more abundant, which is a general trend in the crystallization process: the lower the crystallization temperature, the higher the nucleation density and the smaller the sizes of the crystallites. All of these properties are related to the viscosity of the sample medium and the driving force for segregation. The "B" process was depressed by the competition between the viscosity of the sample medium and the driving force for segregation due to the decrease in temperature. As the crystallization temperature is decreased, the medium viscosity dominates the crystallization process. This trend was more clearly shown by the further decrease in temperature.

Reducing the temperature from 175 to 120 °C first segregates the main chain and side chains, and then the following crystallization process of the main chain further reduces the system enthalpy. This segregation process is opposed by the associated loss in the system entropy. In general, diblock copolymer entropy is inversely proportional to molecular weight, N, and the product χN controls the state of segregation. As the temperature decreases, this parameter further increases over the critical value, which induces the first-order transition to an ordered state. In this case, entropically favored but energetically costly curved and disordered microstructures are exchanged for a periodic mesophase, bilayered lamellar structure. This phase transition is not a true phase transition in the rigorous thermodynamic sense, but the polymer geometry or conformation can undergo dramatic changes over slight temperature changes in a pseudo-first-order manner. Although the structure of poly(3-dodecylthiophene) is not as simple as the diblock structure of the flexible polymers, the order−disorder transition mechanism can be applied to this material. This transition in the P3DDT sample is very limited by the diffusion of the stiff P3DT chains. Our low-temperature data show that the order−disorder transition behavior is more complex than that at 120 °C because of the competition between the driving force for the order−disorder transition and the medium viscosity of the sample.

Figure 6 shows the thermal behavior of P3DDT at 100 °C with a clear double peak. The additional peak at 144 °C is evident after the annealing at 100 °C. The magnitudes of the two peaks are similar as the sample was annealed at 100 °C for 1 min. The lower melting of the double peaks is related to the "B" process and

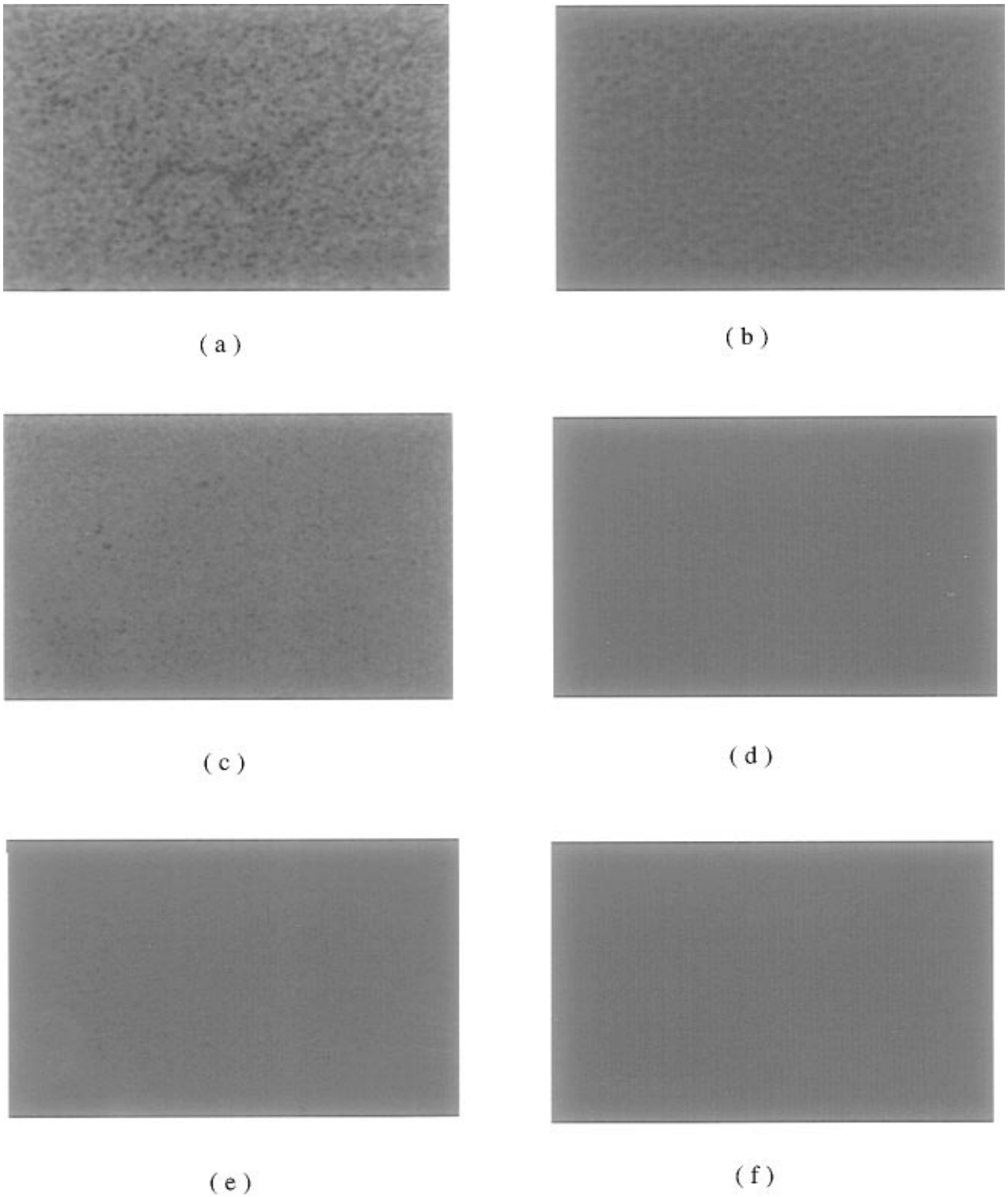

Figure 8. Optical micrographs of poly(3-dodecylthiophene) films crystallized at 110, 100, and 90 °C for different times (magnification, ×300): (a) 110 °C, 15 min; (b) 110 °C, 30 min; (c) 100 °C, 1 min; (d) 100 °C, 5 min; (e) 90 °C, 10 s; (f) 90 °C, 30 s.

the higher peak is related to the "C" process, which represent the isotropization of the less-ordered phase. These relationships are more clearly seen by the comparison with the results of optical microscopy. Parts c and d of Figure 8 show the same trend as shown in Figure 8a,b, but the rate of change is faster than that at 110 °C. Figure 8c clearly shows the red dot structures and deep red color developed for the sample annealed at 100 °C for 1 min. After 5 min, the red dot structures can no longer be seen, as shown in Figure 8d. They have not disappeared, but cannot be detected due the simultaneous "C" process. This implies that the "B" process is decreased at this temperature. It became more difficult for the crystallites to reach their equilibrium state because the medium became more viscous as the annealing temperature was lowered. The "B" phase developed at 100 °C has a broader degree of crystallinity, and the quantity of the "C" process seems to be larger than that at 110 °C.

Figure 7 shows the thermal behavior of the sample annealed at 90 °C. The shape of the DSC thermogram is almost the same as that of the second heating shown in Figure 2. There were no differences among the DSC thermograms annealed at 90 °C for different periods of

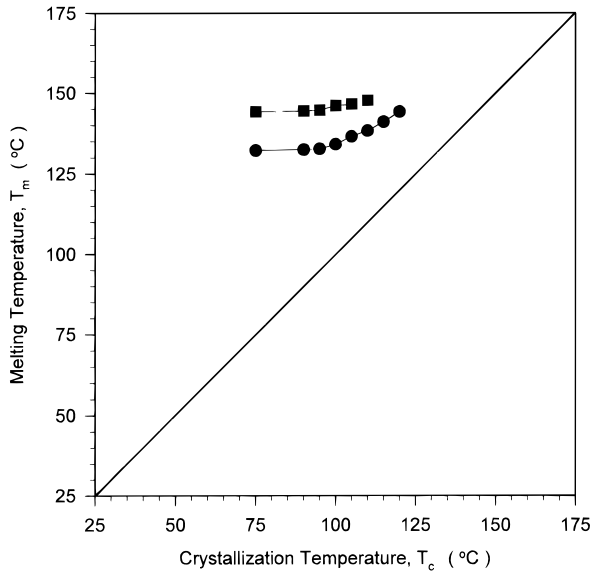

Figure 9. Endothermic peak maxima *vs* crystallization temperature for the samples crystallized at each crystallization temperature for 24 h: (■) isotropization temperature of the less-ordered phase; (●) melting temperature of crystalline phase.

time except that the region below the first melting peak gradually increased as the annealing time was increased. The double peaks appear simultaneously, which implies that the processes are so fast that they could not be separated at 90 °C any more. The above results show that we have been able to differentiate two order formation processes which result in the double melting behavior. The major reason for our observation is the careful investigation at the high-temperature range and slow cooling kinetics. It is obvious that the "B" process occurs at high temperatures first, as evidenced with the red dot structures and single endotherm, and the "C" process, which can be evidenced with the double endotherms and the color change in the background of the red dots, becomes competitive under higher supercooling rates.

Hence, the samples prepared by the general quenching method contain two phases: one is a crystalline phase, and the other is a less-ordered phase. Both phases have the same basic layered structure, but they have different degrees of crystallinity of the main chains. Parts e and f of Figure 8 show the optical microscopy results of the samples annealed at 90 °C for 10 and 30 s, respectively. The sample has a weak dot-like structure, which cannot be seen any more in the sample annealed at 90 °C for 30 s and longer, as shown in Figure 8f. The crystallization process was so restricted at 90 °C that the red dot structure is difficult to see in the series of pictures, although these red dot structures still exist. The series of DSC thermograms confirms the existence of these two phases. These two phase behaviors are the cause of the double peaks appearing in the higher temperature region in the DSC thermograms.

The thermal behaviors of P3DDT at temperatures higher than 120 °C were also investigated. The DSC results did not show any peak for the sample annealed at 130 °C for 24 h, and the optical microscope also did not show any morphological changes. These results imply that the crystallization of the main chains of P3DDT does not occur over 130 °C and that the sample is amorphous at this temperature.

Figure 9 shows the summary of DSC results, which reveals the relationship between the crystallization temperatures and the melting temperatures. All the points were taken from the samples annealed for 24 h at each corresponding temperature. These data show the two-phase behavior of P3DDT systematically. When the annealing temperature is higher than 120 °C, the sample does not show any changes in the DSC and optical microscope results. Hence, this sample seems to have a single phase, or isotropic, where the main chain and side chains act like miscible components. At 120 and 115 °C, DSC results show a single melting peak, which is related to the crystalline phase, and optical micrographs show clear crystallization behavior. In these temperature regions, the sample has a layered, smectic-like, crystalline phase after long annealing. DSC results show two peaks below 110 °C. The lower one is related to the crystalline phase ("B" process) and the higher one is related to the isotropization of the less ordered "C" phase, which is developed by the restriction of crystallization due to the increase of sample viscosity. Two phases were clearly shown below 100 °C with the DSC and optical microscope results, and there were no more changes below 90 °C.

As the annealing temperature increased, the melting temperature of the crystalline phase increased from 132 to 144 °C and the isotropization temperature changed from 144 to 148 °C. When P3DDT is crystallized at temperatures above 120 °C, two peak maxima would coincide and only one peak should be observable. This trend was also reported in poly(3-hexylthiophene) (P3HT) by Leclerc *et al.*, who studied the isothermal crystallization of a P3HT sample over a wide range of temperatures.[26] They observed two well-separated crystal formation processes: a fast one that which produces crystals having higher transition temperatures and a slow process that leads to continuous growth of less stable crystals. We consider that these fast and slow processes correspond to our "C" and "B" processes, respectively. As mentioned above, we concluded that the "B" process produces a well-ordered crystalline phase and leads to continuous growth of crystals and that the "C" process produces a less-ordered phase having a higher melting temperature than the well-ordered phase. This is contrary to the fact that melting temperatures of crystalline materials are proportional to their crystal sizes and degrees of crystallinity in general. We could not completely explain why the well-ordered phase has a lower melting temperature than the less-ordered phase at this point, but we consider that these processes seem to be dominated by entropy changes, as the enthalpy changes between the crystalline state and the melt state are small. Actually, the total enthalpy change of the double peaks in the high-temperature region shown in Figure 2 was about 10.6 J/g (2.7 kJ/mol), which is much less than expected for enthalpy changes normally assigned to crystalline materials on melting. In this case T_m ($=\Delta H_f/\Delta S_f$) is highly dependent on the entropy changes. This is very similar to liquid crystalline behavior in which the smectic phase will occur at a lower temperature in accord with its higher degree of order. Based on these data, there is some possibility that P3DDT can show the liquid crystalline behavior as proposed by others.[4,5] Hence, the thermal behavior of P3DDT was thoroughly investigated to find a liquid crystalline phase, but no liquid crystallinity was observed under the conditions usually applied to thermotropic liquid crystalline materials.

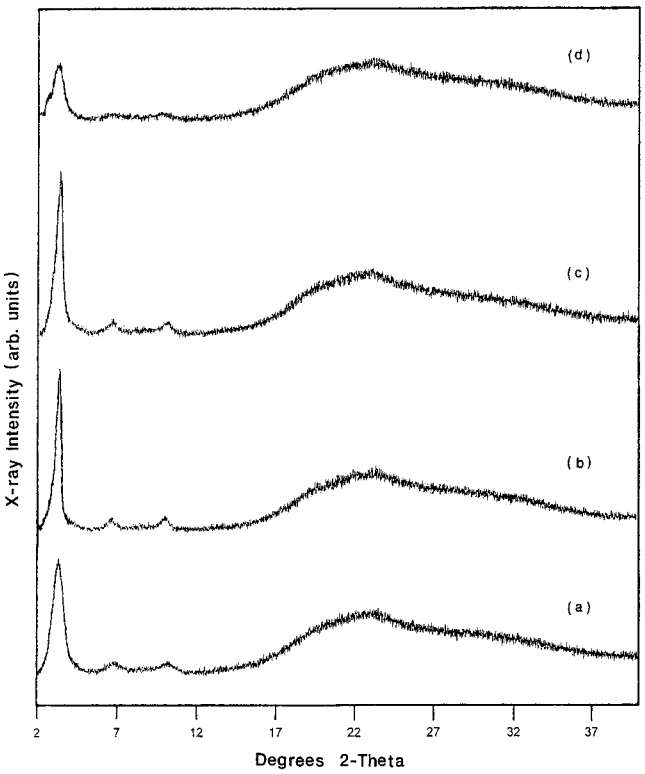

Figure 10. X-ray diffraction profiles of the poly(3-dodecylthiophene): (a) as-cast film; (b) film crystallized at 90 °C for 24 h; (c) film crystallized at 120 °C for 24 h; (d) film quenched from 175 °C.

P3DDT does not show any liquid crystallinity under crossed-polarized conditions. It is not known yet why P3DDT does not show any liquid crystalline texture under crossed-polarized conditions in spite of the crystalline behavior observed by DSC and optical microscopy. The liquid crystallinity of P3DDT under sheared conditions is reported in detail elsewhere.[25]

The X-ray results are shown in Figure 10. The as-cast film in chloroform in Figure 10a shows three scattering peaks clearly located at low angles. These reflections arise from the first- (d = 27.0 Å, 3.27°), the second- (d = 12.7 Å, 6.97°), and the third-order reflections (d = 8.7 Å, 10.20°), as reported previously.[5,27] Parts b and c of Figure 10, which were annealed at 90 and 120 °C, respectively, for 24 h and then quenched by dry ice, show that the first-order peak and higher orders were clearer and sharper than for the solution cast sample. Despite the two phases shown by the optical microscopy and DSC, X-ray results did not show any additional crystalline structure peaks. On the basis of the sharpening and increase in intensity of the first-order peak, it was proposed that the two phases have the same bilayered structure and the only difference is in the degree of crystallization, which means that well-ordered red dot-like structures have compact crystalline structures, while the "C" process results in a less-ordered phase. Figure 10d shows X-ray results of the sample quenched from 175 °C using dry ice. This sample also has a first-order peak representing a bilayered structure, but the reduced intensity of the first-order peak and the absence of higher order peaks implies that the morphology of the quenched sample has a less-ordered structure than that of the as-cast film. The investigators using the regioregular samples have also reported the formation of two different ordered phases.[28−30] The structural analysis resulted in a conclusion very similar to ours, although optical microscopy was not applied. We shall include these regioregular samples in our morphology studies.

IV. Conclusions

In this paper we have thoroughly studied the thermal behaviors of P3DDT using the DSC, optical microscope, and X-ray scattering methods to investigate morphological changes with thermal history and to find which factor is most critical to the thermochromism of this material.

The order−disorder transition of the electroactive polymer P3DDT was first observed under an optical microscope. The micrographs showed that the P3DDT sample contains two phases: one is a well-ordered phase and the other is a less-ordered phase. The red dot structures are well-ordered crystalline parts; they are indicative of the major modification of the electronic structure with an increase in the length of the conjugation segment. This was also confirmed by DSC and X-ray experiments. These experimental results strongly suggest that thermochromism may take place by interchain mechanisms such as crystallization or arrangement of the main chains. Despite the fact that the temperature range from 90 to 120 °C is well above the melting temperature of side chains in both the heating and cooling cycles, the color of the P3DDT changed with the annealing times. This means that the role of the side chains in the thermochromism of P3DDT is not critical, but the main chain arrangement is. The comparison of the DSC results with the optical microscopy results was very helpful in the investigation of the thermal behavior of P3DDT.

References and Notes

(1) Scrosati, B. *Applications of Electroactive Polymers*; Chapman & Hall: London, 1994.
(2) Gustafsson, G.; Cao, Y.; Treacy, G. M.; Klavetter, F.; Colaneri, N.; Heeger, A. J. *Nature* **1992**, *357*, 477.
(3) Prasad, P. N.; Williams, D. J. *Introduction to Nonlinear Optical Effects in Molecules & Polymers*; John Wiley: New York, 1991.
(4) Prosa, T. J.; Winokur, M. J.; Moulton, J.; Smith, P.; Heeger, A. J. *Macromolecules* **1992**, *25*, 4364.
(5) (a) Tashiro, K.; Ono, K.; Minagawa, Y.; Kobayashi, M.; Kawai, T.; Yoshino, K. *J. Polym. Sci., Part B: Polym. Phys. Ed.* **1991**, *29*, 1223. (b) Qian, R.; Chen, S.; Song, W.; Bi, X. *Macromol. Rapid Commun.* **1994**, *15*, 1.
(6) Rughooputh, S. D. D. V.; Hotta, S.; Heeger, A. J.; Wudl, F. *J. Polym. Sci., Part B: Polym. Phys. Ed.* **1987**, *25*, 1071.
(7) Inganäs, O.; Salaneck, W. R.; Österholm, J.-E.; Laakso, J. *Synth. Met.* **1988**, *22*, 395.
(8) Jen, K. Y.; Miller, G. G.; Elsenbaumer, R. L. *J. Chem. Soc., Chem. Commun.* **1986**, 1346.
(9) Hotta, S.; Rughooputh, S. D. D. V.; Heeger, A. J.; Wudl, F. *Macromolecules* **1987**, *20*, 212.
(10) Bates, F. S.; Rosedale, J. H.; Fredrickson, G. H. *J. Chem. Phys.* **1990**, *92*, 6255.
(11) Leibler, L. *Macromolecules* **1980**, *13*, 1602.
(12) Bates, F. S. *Science* **1991**, *251*, 898.
(13) Lim, K. C.; Heeger, A. J. *J. Chem. Phys.* **1985**, *82*, 522.
(14) Wenz, G.; Müller, M. A.; Schmidt, M.; Wegner, G. *Macromolecules* **1984**, *17*, 837.
(15) Harrah, L. A.; Zeigler, J. M. *J. Polym. Sci., Polym. Lett. Ed.* **1985**, *23*, 209.
(16) Trefonas, P.; Damewood, J. R.; West, R.; Miller, R. D. *Organometallics* **1985**, *4*, 1318.
(17) Shukla, P.; Cotts, P. M.; Miller, R. D.; Russell, T. P.; Smith, B. A.; Wallraff, G. M.; Baier, M. *Macromolecules* **1991**, *24*, 5606.
(18) Chance, R. R.; Patel, G. N.; Witt, J. D. *J. Chem. Phys.* **1979**, *71*, 206.
(19) Miller, R. D.; Hofer, D.; Rabolt, J. *J. Am. Chem. Soc.* **1985**, *107*, 2172.

(20) Berlinsky, A. J.; Wudl, F.; Lim, K. C.; Fincher, C. R.; Heeger, A. J. *J. Polym. Sci., Polym. Phys. Ed.* **1984**, *22*, 847.
(21) Patel, G. N.; Chance, R. R.; Witt, J. D. *J. Chem. Phys.* **1979**, *70*, 4387.
(22) Schweizer, K. S. *J. Chem. Phys.* **1986**, *85*, 1156.
(23) Schweizer, K. S. *J. Chem. Phys.* **1986**, *85*, 1176.
(24) (a) Ho, K.; Bartus, J.; Levon, K.; Mao, J.; Zheng, W.; Laakso, J.; Taka, T. *Synth. Met.* 384. (b) Zheng, W.-Y.; Levon, K.; Laakso, J.; Österholm, J.-E. *Macromolecules* **1994**, *27*, 7754. (c) Kim, H. K. Competition between the side chain crystallization and the ordering of the main chain in poly(3-alkylthiophene)s. Ph.D. Thesis, Polytechnic University, 1994.
(25) Park, K. C.; Levon, K. To be submitted for publication.
(26) Zhao, Y.; Yuan, G.; Roche, P.; Leclerc, M. *Polymer* **1995**, *36*, 2211.
(27) Chen, S.-A.; Ni, J.-M. *Macromolecules* **1992**, *25*, 6081.
(28) Faid, K.; Frechette, M.; Ranger, M.; Mazerolle, L.; Levesque, I.; Leclerc, M.; Chen, T.-A.; Rieke, R. D. *Chem. Mater.* **1995**, *7*, 1390.
(29) McCullough, R. D.; Low, R. D.; Jayaraman, M.; Anderson, D. L. *J. Org. Chem.* **1993**, *58*, 904.
(30) Yang, C.; Orfino, F. P.; Holdcroft, S. *Macromolecules* **1996**, *29*, 6510.

MA961322J